AD-A036 331 AIR FORCE GEOPHYSICS LAB HANSCOM AFB MASS F/G 7/4
HIGH-RESOLUTION SPECTRA OF CH4 IN THE 2700 TO 3200 CM-1 REGION.(U)
NOV 76 H SAKAI

UNCLASSIFIED AFGL-TR-76-0280 NL

| OF |

AD
A036331

END

DATE
FILMED
3-77

(12)

AFGL-TR-76-0280
ENVIRONMENTAL RESEARCH PAPERS, NO. 584

High-Resolution Spectra of CH_4 in the 2700 to 3200 cm^{-1} Region

HAJIME SAKAI

29 November 1976

OPTICAL PHYSICS DIVISION PROJECT 2310
AIR FORCE GEOPHYSICS LABORATORY
HANSCOM AFB, MASSACHUSETTS 01731

AIR FORCE SYSTEMS COMMAND, USAF

This report has been reviewed by the ESD Information Office (OI) and is releasable to the National Technical Information Service (NTIS).

This technical report has been reviewed and is approved for publication.

FOR THE COMMANDER

John Howard

Chief Scientist

Qualified requestors may obtain additional copies from the Defense Documentation Center. All others should apply to the National Technical Information Service.

Unclassified
SECURITY CLASSIFICATION OF THIS PAGE (When Data Entered)

REPORT DOCUMENTATION PAGE		READ INSTRUCTIONS BEFORE COMPLETING FORM
1. REPORT NUMBER 14 AFGL-TR-76-0280, AFGL-ERP-584	2. GOVT ACCESSION NO.	3. RECIPIENT'S CATALOG NUMBER
4. TITLE (and Subtitle) 6 HIGH-RESOLUTION SPECTRA OF CH_4 IN THE 2700 to 3200 cm^{-1} REGION		5. TYPE OF REPORT & PERIOD COVERED Scientific. Interim.
		6. PERFORMING ORG. REPORT NUMBER ERP No. 584
7. AUTHOR(s) 10 Hajime Sakai		8. CONTRACT OR GRANT NUMBER(s) 12 21p.
9. PERFORMING ORGANIZATION NAME AND ADDRESS Air Force Geophysics Laboratory (OPI) Hanscom AFB, Massachusetts 01731	16	10. PROGRAM ELEMENT, PROJECT, TASK AREA & WORK UNIT NUMBERS 61102F 2310G101 17 G1
11. CONTROLLING OFFICE NAME AND ADDRESS Air Force Geophysics Laboratory (OPI) Hanscom AFB, Massachusetts 01731	11	12. REPORT DATE 29 Nov[redacted]76
		13. NUMBER OF PAGES 20
14. MONITORING AGENCY NAME & ADDRESS (if different from Controlling Office) 9 Environmental research papers,		15. SECURITY CLASS. (of this report) Unclassified
		15a. DECLASSIFICATION DOWNGRADING SCHEDULE

16. DISTRIBUTION STATEMENT (of this Report)

Approved for public release; distribution unlimited.

17. DISTRIBUTION STATEMENT (of the abstract entered in Block 20, if different from Report)

18. SUPPLEMENTARY NOTES

19. KEY WORDS (Continue on reverse side if necessary and identify by block number)

Methane
Fourier
Spectroscopy

20. ABSTRACT (Continue on reverse side if necessary and identify by block number)

The Idealab 2-m path-difference interferometer was used to obtain data of CH_4 in the 2700 to 3200 cm^{-1} region to a resolution of 0.006 cm^{-1}. Obtained spectral data are presented as well as the results of analysis to calculate line positions and strengths. A comparison of the present data with previously obtained data is also presented. The results of this study are tabulated using the format of the AFGL atmospheric line compilation.

DD FORM 1 JAN 73 1473 EDITION OF 1 NOV 65 IS OBSOLETE

Unclassified
SECURITY CLASSIFICATION OF THIS PAGE (When Data Entered)

* 1/2700 to 1/3200 cm 1/.006 cm

409 578

Unclassified

SECURITY CLASSIFICATION OF THIS PAGE(*When Data Entered*)

Unclassified

SECURITY CLASSIFICATION OF THIS PAGE(*When Data Entered*)

2

Contents

Illustrations

Tables

High-Resolution Spectra of CH_4 In the 2700 to 3200 cm^{-1} Region

1. INTRODUCTION

The AFGL atmospheric line compilation contains the line parameters of the infrared methane bands.[1] The work on methane was started by Kyle and later revised by Fox.[2] The compilation of methane is rather extensive, covering most of the major infrared bands; however, it is still considered incomplete. The most intense band of methane in the infrared region is the so-called ν_3 band (00011001 – 00000000 transition according to the designation used in the AFGL line compilation) of $C^{12}H_4$, extending in spectral range from 2700 cm^{-1} to 3200 cm^{-1}. The line data for this band are compiled from both existing experimental data and theoretical analysis. Other methane bands, which are weaker than the ν_3 band of $C^{12}H_4$ but make a significant contribution to infrared absorption in this region, are the ν_3 of $C^{13}H_4$ (00011001 – 00000000) and the $(\nu_2 + \nu_4)$ of $C^{12}H_4$ (0110112 – 00000000). The calculated strength of lines in these bands, which are in the compilation, ranges from 10^{-23} to $2x10^{-19}$ in units of $cm^{-1}/(molecules\ cm^{-2})$.

The methane spectrum in this spectral range (2700 → 3200 cm^{-1}) exhibits a somewhat complex structure. If the spectroscopic measurement is made to resolve

(Received for publication 24 November 1976)

1. McClatchey et al (1973) AFCRL Atmospheric Absorption Line Parameters Compilation, AFCRL-TR-73-0096.
2. Fox, K. (1973) Analysis of Vibration-Rotation Spectra of Methane, AFCRL-TR-73-0738.

all the spectral lines, the resolution of the spectrometer must be at least as fine as the Doppler width of these lines, that is, 0.0047 cm^{-1}. Our 2-m path-difference interferometer spectrometer[3,4] is capable of producing the required resolution. The present work was accomplished to achieve two goals: testing the performance capability of our interferometer, and examining the line parameters compiled for the 3-μ methane lines in the AFGL atmospheric line compilation.

Traditionally, the spectral analysis has been mainly concerned with the determination of line positions in the measured spectral band. On the other hand, very little has been done in the way of analysis of measured line strengths and widths of individually measured lines. The present work was undertaken to devise an automatic computation program for analyzing line strengths and widths as well as for determining line positions.

2. EXPERIMENTAL PART

The interferometer spectrometer used for the present measurement has been described in previous reports, together with the scheme for recording the interferogram function.[3,4] The computational method used in processing the interferogram data to obtain the spectrum was also described in the above reports; consequently, no detailed description of it will be presented here. The description that follows highlights those features that are pertinent to the present specific measurement.

The interferometer, with its auxiliary optical components, is housed in a vacuum chamber. Figure 1 is a schematic diagram showing the arrangement. The radiation from the primary source, which is a small tungsten-filament incandescent lamp GE 51, is first focused on a blade of a vibrating reed chopper driven at a rate of 450 Hz. A spectral bandpass filter is placed between the source and the chopper to isolate the spectral region of interest. The chopped beam is refocused at the 1-mm-diam entrance aperture, and then collimated using all-reflecting optics. A 10-cm-long absorption cell, made of fused quartz, is placed before the interferometer and in the path of the collimated beam. Two PbS detectors operating at liquid nitrogen temperature are placed at both output ends of the interferometer to observe the complementary modulations of the interferogram signals. The 6329 Å line from the frequency-stabilized He-Ne cw laser supplies the reference signal used to control the interferometer stepping and the interferogram data sampling. No correction is needed to the measured line position, since the whole

3. Pritchard et al (1973) Two-Meter Path Difference Interferometer for Fourier Spectroscopy, AFCRL-TR-73-0223.
4. Sakai, H. (1974) High-Resolution Fourier Spectroscopy, AFCRL-TR-74-0571.

interferometer system is under vacuum and the atmosphere does not influence the calibration.

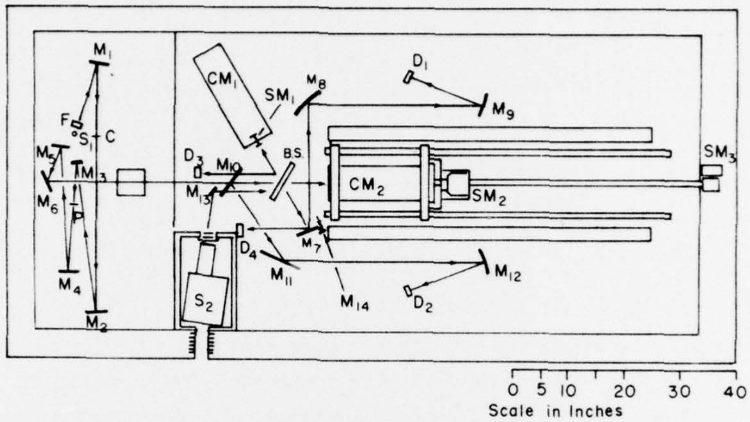

Figure 1. Optical Layout of Interferometer and its Auxiliary Optics. CM_1: stationary cat's eye; CM_2: movable cat's eye; SM_1: piezo-electric crystal transducer; SM_2: magnetic motor; SM_3: printed circuit motor; S_1: signal sources; S_2: reference laser; C: chopper; F: filter; P: entrance hole; D_3 and D_4: *interference fringe signal detectors;* B. S.: beam splitter plate; D_1 and D_2: interferogram signal detectors; Ms: mirrors

The scheme used for recording the interferogram data is shown in Figure 2. The detectors are carefully positioned to produce optimum balance of their output modulations. After these outputs are individually amplified, they are subtracted from each other to yield an interferogram signal that is modulated about zero voltage. An analog phase-adjusting circuit is inserted in one channel, prior to the differencing amplifier, to improve signal balancing. An analog-to-digital converter is used to convert the interferogram signal into a series of digital numbers. The PDP 8e minicomputer performs the arithmetic operations on these digitized values, the operations being equivalent to synchronous demodulation and integration. The interferogram data thus obtained are recorded on digital magnetic tape and processed at the central-site large-scale CDC 6600 computer. The overall dynamic range in this recording scheme is better than 18 bits (approximately 2.6×10^5).

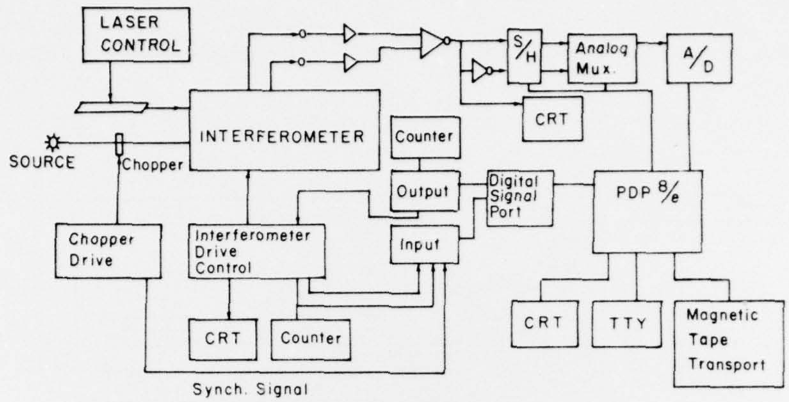

Figure 2. Block Diagram of Data Acquisition System

The methane gas used in the present measurement was of Linde cp grade. The amount of methane in the absorption cell was measured using a Texas Instrument quartz spiral pressure gauge and an oil manometer. The stepping distance of the interferometer was set to twice the wavelength of the He-Ne laser line, which means that the interferogram signal was sampled at every 2×6329.9 Å = 12659.8 Å. The measurement of a complete interferogram took about 10 hr, covering an optical path difference of 100 cm. The hold time of the liquid-nitrogen-detector dewar limits the total measurement time to about 10 hr. The measurements were carried out either at night on workdays or on weekends, in order to avoid the harmful disturbances that we cannot eliminate under normal workday conditions.

The spectral range covered in a single measurement was approximately from 2700 cm^{-1} to 3200 cm^{-1}. As mentioned above, a spectral bandpass filter was used to isolate this spectral region. The recorded interferogram contained about 10^6 data points, which is considerably more than necessary to satisfy the sampling theorem.

Figure 3 shows typical methane spectral data obtained by Fourier-transforming the recorded interferogram data. The spectrum represents the Q branch region of the $C^{12}H_4$ ν_3 band. The periodic modulation of the peak power observed in the spectrum is channelled spectrum, caused by the spectral bandpass filter. The spectral resolution, which corresponds to the distance between adjacent independent spectral data points, is 0.006 cm^{-1}, corresponding to a maximum optical path difference of 90 cm. Table 1 summarizes the experimental conditions under which data were taken for the present analysis.

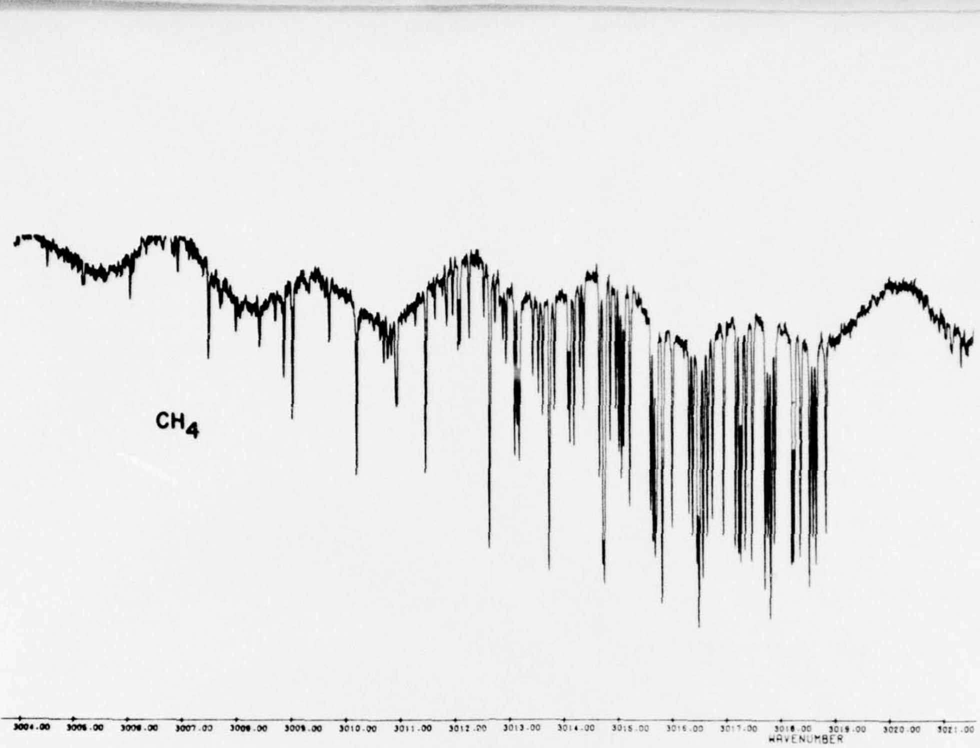

Figure 3. Raw Methane Absorption Spectrum

Table 1. Summary of the Data Runs Taken for Various Methane Pressures (Absorption cell length = 10 cm)

Methane Pressure in mm Hg	No. of Runs
1.0	4
1.6	4
2.5	1
2.7	6
9.0	1
21.0	1

3. DATA ANALYSIS

Analysis of the spectral data was carried out according to the sequence shown in the flow diagram of Figure 4. The absorptance spectrum produced by the first stage program is shown in Figure 5. In the next stage the positions of all absorption peaks were determined to an accuracy better than 1/8 of the spectral resolution. The last stage of the sequence was to determine the strengths and widths of all observed lines, using the least-square-error curve-fitting algorithm. In constructing the last stage algorithm, the following assumptions were made: (1) the lines may be characterized as having a Doppler-broadened Gaussian shape; (2) all lines are free of severe overlapping so that the observed peaks correspond to the centers of the lines; and (3) all lines are not strongly saturated at their absorption peaks. The algorithm was able to produce the strengths and widths of each constituent line, even in the case where the lines being analyzed overlapped somewhat.

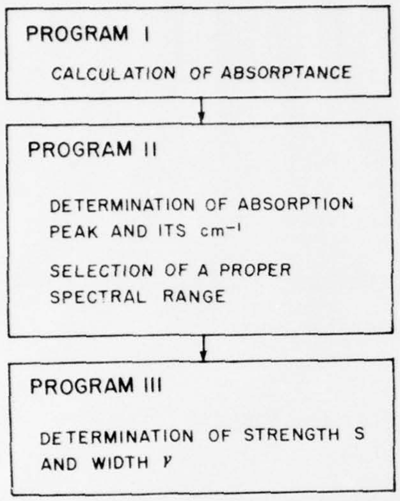

Figure 4. Flow Diagram of Spectral Data Analysis

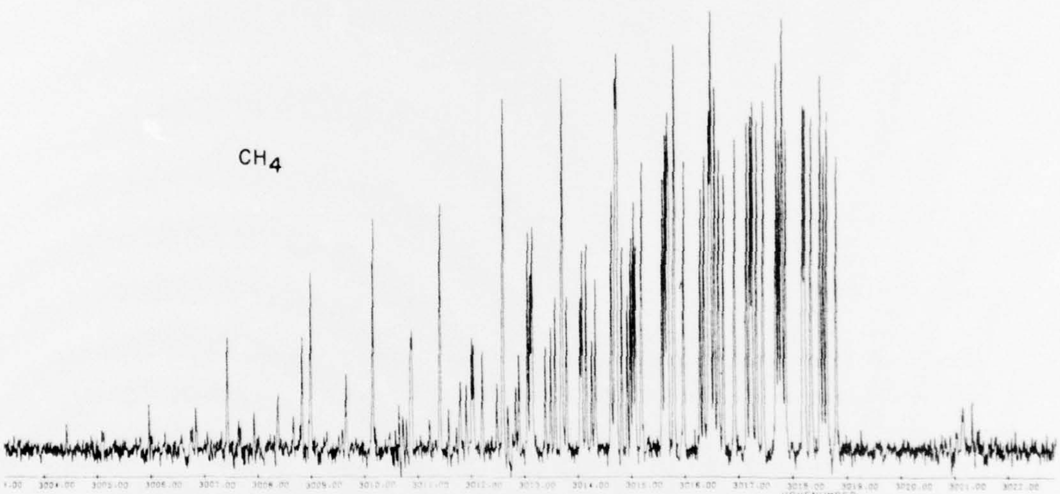

Figure 5. CH_4 Absorptance Spectrum

The first assumption is considered appropriate, since the pressured ranges used for all the measurements were quite low. The intermolecular collisions in those pressure ranges do not produce any significant line broadening. The widths determined for most of the data were not too different from the theoretically calculated value of 0.0047 cm^{-1}. Thus, there is no indication of inconsistency between the assumptions and the results obtained.

The second assumption can be tested by examining the widths determined from the analysis. An unusually large value of line widths compared with those determined for neighboring lines would indicate the presence of hidden lines, even if the observed data suggest a single line. This was not the case for most of the data observed, except for the forbidden Q^+ branch where the blending is quite severe.

The third assumption is the most crucial one for deciding on the applicability of the algorithm. It was found that the algorithm failed to produce a unique set of solutions for the strengths and widths of lines that are too strong. Once the absorption coefficient at the line center exceeds a certain threshold value, interdependency between these two parameters becomes too high to allow independent determination of the strength and width. Iterative application of the least-square curve-fitting computation for this case fails to produce a convergent set of solutions. This difficulty can be avoided by selecting the appropriate range of pressures for the analysis of individual lines. The stronger lines were analyzed using the low pressure data, while the weaker lines were processed using the high pressure data.

The line parameter data produced from data from each interferogram were normalized according to the methane concentration present in the absorption cell. The data obtained from all interferograms were collected for the individual lines and averaged. Figure 6 shows a comparison between one of the observed absorptance spectrum and the spectrum calculated for the same methane concentration using the line parameters resulting from analysis of the present data. The agreement between these two spectra is adequate to conclude that the line parameters determined in this work are acceptable and within experimental error for the present measurement.

Figure 7 shows a comparison between the observed absorptance spectrum and that synthesized from the line parameters compiled by Fox. It can be seen that the band head section of the Q branch shows satisfactory agreement. Discrepancy between these two spectra is noticeable, however, in the region below 3013 cm^{-1}, where the lines are due to transitions between levels corresponding to high rotational quantum numbers.

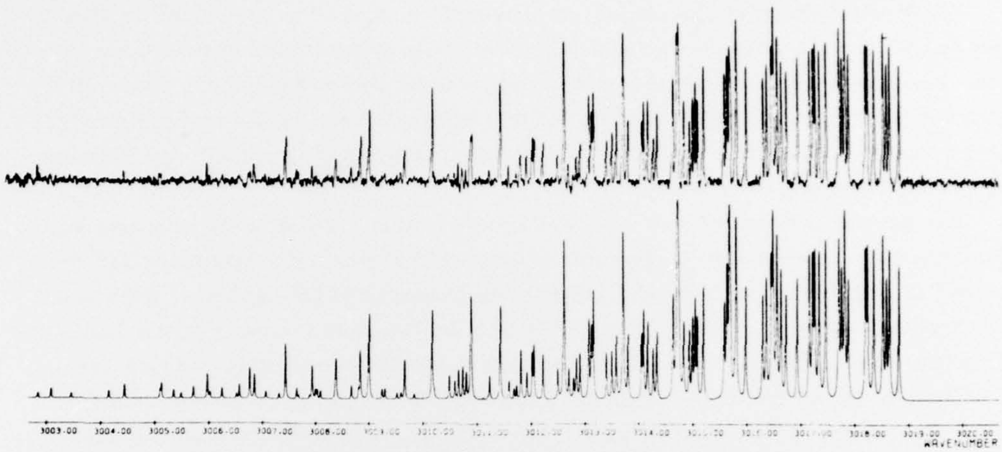

Figure 6. Comparison of Observed CH_4 Absorptance Spectrum With Synthetic Spectrum Calculated Using the Line Parameters Derived From Present Analysis

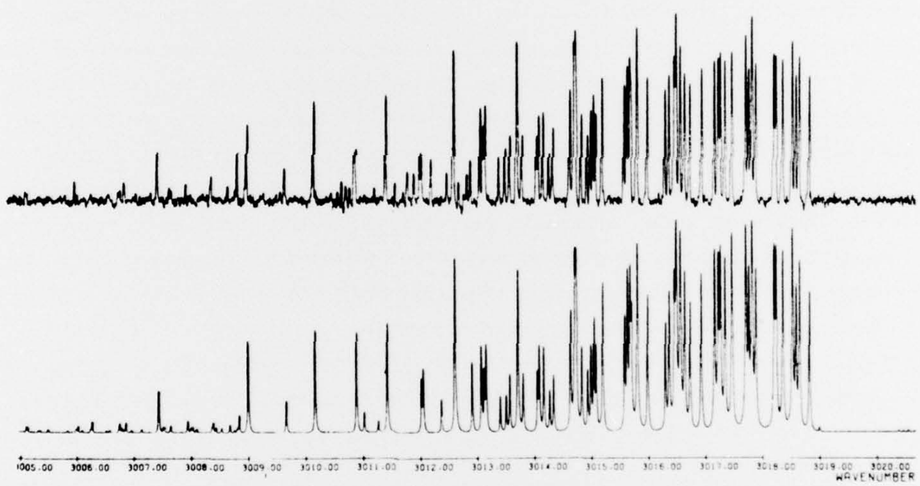

Figure 7. Comparison of Observed CH_4 Absorptance Spectrum With Synthetic Spectrum Calculated Using the Line Parameters Compiled by Fox

4. RESULTS AND DISCUSSION

The results of this study are listed in Table 2, using the format of the AFGL atmospheric line compilation (F10.3, E10.3, F5.3, F10.3, 2A9, 2A8, 2I4, I3). The lines are usually identified according to the line listing compiled by Fox. Values for the widths are left blank, since the present work essentially only measured the Doppler-broadened width. As indicated in Figure 7, the line compilation for the spectral range of 3000 cm^{-1} to 3013 cm^{-1} is unsatisfactory. Of the lines observed in this spectral range, identification is assigned only to those lines that show good agreement with the line compilation. The unidentified lines show a blank space between column 27 and 77. The values of the lower energy levels in the present list are taken from the recent French work.[5] The internal identification code that appears from column 81 through 84 is 36 for the present result. The lines for the forbidden Q^+ branch in the range around 3020 cm^{-1} are those compiled by Fox, and are indicated by the code 73. The analysis of these lines was not attempted because of their severe overlapping. Several other $C^{12}H_4$ lines of the ν_3 band are also left unanalyzed, because of the same difficulty. Those lines are listed in Table 3.

After the major portion of the present work had been completed, but before this report was written, work by Pine was published.[6] He measured the major $C^{12}H_4$ lines of the ν_3 band between 2916 cm^{-1} and 3123 cm^{-1} using the tunable laser technique. The spectral resolution that he attained using the laser technique is better than $10^{-4}cm^{-1}$. The signal-to-noise ratio of his measurement is significantly better than that of the present measurement. The line strength values obtained by Pine for those lines are slightly higher than the values compiled by Fox (about 20 to 30 percent), while the values obtained by the present work average around the Fox values.

---

5. Tarrago et al (1976) J. Mol. Spectrosc., 57:246.
6. Pine, A.S. (1976) J. Opt. Soc. Am., 66:97.

Table 2. Results Obtained

2894.996	.131E-19	815.144	00 11001	00000000	1112A21	1212A11	36	211	6
2895.057	.573E-20	815.132	00 11001	00000000	1112F21	1212F11	36	211	6
2895.129	.554E-20	815.116	00 11001	00000000	1112F11	1212F21	36	211	6
2895.233	.126E-19	815.089	00 11001	00000000	1112A11	1212A21	36	211	6
2895.759	.120E-19	815.008	00 11001	00000000	1112F12	1212F22	36	211	6
2895.827	.440E-20	814.993	00 11001	00000000	1112 E1	1212 E1	36	211	6
2896.202	.576E-20	814.884	00 11001	00000000	1112F22	1212F12	36	211	6
2896.300	.100E-19	814.847	00 11001	00000000	1112F13	1212F23	36	211	6
2896.983	.329E-19								6
2897.404	.156E-20								6
2898.695	.115E-20								6
2899.323	.126E-20								6
2899.932	.916E-21								6
2900.119	.846E-20	62.878	01100112	00000000	4 3A11	5 3A21	36	211	6
2901.539	.214E-20	62.876	01100112	00000000	4 3F21	5 3F11	36	211	6
2901.887	.329E-20								6
2903.875	.695E-21								6
2904.529	.946E-21								6
2905.633	.128E-19	690.049	00 11001	00000000	1011F23	1111F13	36	211	6
2905.699	.670E-20	690.040	00 11001	00000000	1011 E2	1111 E2	36	211	6
2905.813	.176E-19	690.018	00 11001	00000000	1011F13	1111F23	36	211	6
2906.093	.693E-21	575.223	00 11001	00000000	910A21	1010A11	36	311	6
2906.282	.131E-19	689.957	00 11001	00000000	1011F22	1111F12	36	211	6
2906.588	.943E-20	689.886	00 11001	00000000	1011 E1	1111 E1	36	211	6
2906.649	.137E-19	689.877	00 11001	00000000	1011F 2	1111F22	36	211	6
2906.735	.187E-19	689.862	00 11001	00000000	1011A11	1111A21	36	211	6
2907.325	.315E-19								6
2908.331	.211E-20								6
2909.273	.252E-20								6
2909.884	.147E-20								6
2910.554	.301E-20								6
2910.812	.736E-21								6
2913.788	.824E-21								6
2914.921	.603E-21								6
2916.001	.304E-20								6
2916.007	.214E-20								6
2916.201	.150E-19	575.295	00 11001	00000000	910F11	1010F21	36	211	6
2916.302	.127E-19	575.272	00 11001	00000000	910 E1	1010 E1	36	211	6
2916.395	.274E-19	575.260	00 11001	00000000	910F21	1010F11	36	211	6
2916.524	.180E-20								6
2916.753	.265E-19	575.223	00 11001	00000000	910A21	1010A11	36	211	6
2916.966	.187E-19	575.194	00 11001	00000000	910F22	1010F12	36	211	6
2917.065	.212E-19	575.170	00 11001	00000000	910F12	1010F22	36	211	6
2917.63[illegible]	.285E-19	575.056	00 11001	00000000	910A11	1010A21	36	211	6
2918.485	.143E-20								6
2918.735	.357E-20								6
2919.132	.700E-20								6
2919.891	.109E-20								6
2920.195	.515E-21								6
2920.616	.715E-21								6
2920.665	.120E-20								6
2921.333	.952E-21								6
2922.911	.537E-21								6
2923.949	.262E-21								6
2926.700	.504E-19	470.973	00 11004	00000000	8 9A11	9 9A21	36	211	6
2926.782	.241E-19	470.865	00 11004	00000000	8 9F12	9 9F22	36	211	6
2926.885	.237E-19	470.855	00 11001	00000000	8 9F23	9 9F13	36	211	6
2927.075	.440E-19	470.831	00 11001	00000000	8 9A21	9 9A11	36	211	6
2927.372	.233E-19	470.805	00 11001	00000000	8 9F22	9 9F12	36	211	6
2927.429	.188E-19	470.799	00 11001	00000000	8 9 E1	9 9 E1	36	211	6

Table 2. Results Obtained (Cont)

2927.044	.473E-21	376.730	00	11001	000000_0	7	8A12	5	8A11	36	311	6
2927.932	.335E-19	479.720	00	11001	000000_0	8	9F11	4	9F21	36	211	6
2927.964	.212E-19	479.717	00	11001	000000_0	8	9F21	4	9F11	36	211	6
2931.744	.273E-20	157.139	01	00112	000000_0	6	5F22	5	5F12	36	211	6
2931.962	.240E-21	376.734	00	11001	000000_0	7	7F21	5	8F12	36	211	6
2931.992	.173E-21											6
2932.023	.347E-21											6
2932.251	.177E-20	157.137	01	00112	000000_0	6	5 E1	5	5 E1	36	211	6
2935.85	.305E-20	157.128	01	00112	000000_0	6	5F11	5	5F21	36	211	6
2935.24	.317E-20	157.124	01	00112	000000_0	6	5F21	5	5F11	36	211	6
2937.234	.464E-19	376.820	00	11001	000000_0	7	8F11	5	8F21	36	211	6
2937.302	.202E-19	376.821	00	11001	000000_0	7	8 E1	5	8 E1	36	211	6
2937.494	.354E-19	376.815	00	11001	000000_0	7	8F21	5	8F11	36	211	6
2937.655	.225E-21	293.154	00	11001	000000_0	6	7A11	7	7A21	36	311	6
2937.756	.385E-19	376.780	00	11001	000000_0	7	8F12	5	8F22	36	211	6
2937.913	.304E-21	293.120	00	11001	000000_0	6	7F11	7	7F21	36	311	6
2937.967	.304E-21	293.123	00	11001	000000_0	6	7F21	7	7F11	36	311	6
2938.195	.450E-19	376.735	00	11001	000000_0	7	8 E2	5	8 E2	36	211	6
2938.214	.592E-19	376.734	00	11001	000000_0	7	8F22	5	8F12	36	211	6
2938.25	.404E-19	376.730	00	11001	000000_0	7	8A21	5	8A11	36	211	6
2943.2	.728E-21											6
2943.24	.634E-21											6
2943.332	.244E-20											6
2943.61	.240E-21											6
2943.8	.860E-21											6
2945.04	.585E-21											6
2945.943	.415E-20											6
2946.002	.955E-22											6
2947.425	.152E-20											6
2947.667	.504E-19	293.178	00	11001	000000_0	6	7F22	7	7F12	36	211	6
2947.811	.303E-19	293.170	00	11001	000000_0	6	7 E1	7	7 E1	36	211	6
2947.912	.509E-19	293.164	00	11001	000000_0	6	7F12	7	7F22	36	211	6
2948.197	.100E-18	293.154	00	11001	000000_0	6	7A11	7	7A21	36	211	6
2948.232	.413E-21											6
2948.42	.577E-19	293.126	00	11001	000000_0	6	7F11	7	7F21	36	211	6
2948.474	.455E-19	293.123	00	11001	000000_0	6	7F21	7	7F11	36	211	6
2949.088	.417E-21											6
2949.125	.244E-20											6
2950.343	.409E-21											6
2952.129	.448E-21											6
2953.195	.544E-20	219.920	01	00112	000000_0	7	6A11	5	6A21	36	211	6
2953.539	.327E-20	219.917	01	00112	000000_0	7	6F11	5	6F21	36	211	6
2953.68	.197E-20	219.913	01	00112	000000_0	7	6 E1	5	6 E1	36	211	6
2954.344	.154E-21											6
2954.459	.935E-21	219.915	00	11001	000000_0	5	5F11	6	6F22	36	211	6
2958.017	.103E-18	219.945	00	11001	000000_0	5	6A21	5	6A11	36	211	6
2958.12	.662E-19	219.941	00	11001	000000_0	5	6F21	5	6F11	36	211	6
2958.233	.605E-19	219.937	00	11001	000000_0	5	6F11	5	6F21	36	211	6
2958.427	.390E-21	157.128	00	11001	000000_0	4	5F11	5	5F21	36	311	6
2958.535	.106E-18	219.920	00	11001	000000_0	5	6A11	5	6A21	36	211	6
2958.651	.739E-19	219.915	00	11001	000000_0	5	6F12	5	6F22	36	211	6
2958.682	.193E-19	219.913	00	11001	000000_0	5	6 E1	5	6 E1	36	211	6
2960.95	.128E-20											6
2964.866	.109E-20											5
2964.958	.137E-20											5
2965.524	.494E-21											5
2965.866	.514E-21											5
2966.108	.420E-20											6
2968.492	.775E-19	157.139	00	11001	000000_0	4	5F22	5	5F12	36	211	6
2968.473	.414E-19	157.137	00	11001	000000_0	4	5 E1	5	5 E1	36	211	6

Table 2. Results Obtained (Cont)

2968.735	.770E-19	157.128	00	11001	000000_0	4 5F11	5 5F21	36 211	6
2968.855	.761E-19	157.124	00	11001	000000_0	4 5F21	5 5F11	36 211	6
2971.076	.212E-20	293.120	01	10012	000000_0	8 7F11	7 7F21	36 211	6
2971.283	.212E-20	293.123	01	10012	000000_0	8 7F21	7 7F11	36 211	6
2975.142	.444E-21								5
2976.451	.670E-21								6
2978.649	.103E-18	104.780	00	11001	000000_0	3 4F11	4 4F21	36 211	6
2978.847	.419E-19	104.770	00	11001	000000_0	3 4 E1	4 4 E1	36 211	5
2978.919	.864E-19	104.775	00	11001	000000_0	3 4F21	4 4F11	36 211	6
2979.016	.147E-18	104.773	00	11001	000000_0	3 4A21	4 4A11	36 211	5
2980.073	.813E-21								6
2981.462	.203E-20								5
2982.633	.167E-20								5
2983.385	.130E-20								5
2987.883	.623E-21								6
2988.795	.119E-18	62.876	00	11001	000000_0	2 3A11	3 3A21	36 211	6
2988.932	.744E-19	62.877	00	11001	000000_0	2 3F11	3 3F21	36 211	5
2989.032	.690E-19	62.876	00	11001	000000_0	2 3F21	3 3F11	36 211	5
2989.083	.291E-20	376.835	01	10012	000000_0	9 9F21	8 8F11	36 211	6
2993.177	.440E-21								5
2994.472	.750E-21								6
2996.865	.100E-20								5
2997.946	.163E-20								5
2998.357	.437E-21								6
2998.993	.403E-19	31.442	00	11001	000000_0	1 2F11	2 2F21	36 211	5
2999.061	.253E-19	31.442	00	11001	000000_0	1 2 E1	2 2 E1	36 211	5
2999.322	.540E-21								6
3000.289	.763E-21								6
3000.734	.174E-21								5
3002.852	.480E-21								5
3003.097	.129E-20								5
3004.465	.440E-21								6
3004.159	.800E+21								6
3004.456	.192E-20	575.170	00	11001	000000_0	1010F12	1010F22	36 311	6
3004.925	.950E-22	575.223	00	11001	000000_0	1010A21	1010A11	36 311	5
3005.108	.981E-21								5
3005.133	.257E-20								6
3005.359	.113E-20	470.895	00	11001	000000_0	9 9F22	9 9F12	36 311	6
3005.504	.417E-21	470.831	00	11001	000000_0	9 9A21	9 9A11	36 311	5
3005.727	.100E-20								5
3005.983	.635E-20	293.123	00	11001	000000_0	7 7F21	7 7F11	36 311	6
3006.253	.254E-21	376.835	00	11001	000000_0	8 8F21	8 8F11	36 311	6
3006.525	.640E-21	376.821	00	11001	000000_0	8 8 E1	8 8 E1	36 311	5
3006.582	.227E-20	376.820	00	11001	000000_0	8 8F11	8 8F21	36 311	6
3006.759	.180E-20								5
3006.774	.540E-20								6
3006.862	.380E-20								6
3007.077	.100E-20								6
3007.144	.877E-21	293.178	00	11001	000000_0	7 7F22	7 7F12	36 311	6
3007.449	.140E-19								5
3007.655	.130E-20	219.965	00	11001	000000_0	6 6A21	6 6A11	36 311	6
3007.691	.301E-21								6
3007.949	.104E-19	104.773	00	11001	000000_0	4 4A21	4 4A11	36 311	5
3008.013	.110E-20	157.159	00	11001	000000_0	5 5F22	5 5F12	36 311	6
3008.039	.974E-21	104.775	00	11001	000000_0	4 4F21	4 4F11	36 311	5
3008.385	.520E-20	104.780	00	11001	000000_0	4 4F11	4 4F21	36 311	5
3008.397	.900E-20	1251.221	00	11001	000000_0	1515A11	1515A21	36 211	5
3008.541	.290E-21	62.877	00	11001	000000_0	3 3F11	3 3F21	36 311	5
3008.815	.180E-20	31.442	00	11001	000000_0	2 2F11	2 2F21	36 311	5
3008.849	.120E-19								5

Table 2. Results Obtained (Cont)

3009.015	.247E-19	13.442	00	11001	00000000	0 1F21	1 1F11	36 211	6
3009.253	.190E-20								6
3009.394	.140E-20								6
3009.533	.124E-20								6
3009.697	.114E-20								6
3009.874	.892E-20								6
3009.849	.793E-21								6
3009.894	.473E-21								6
3010.177	.292E-19								6
3010.219	.799E-21								6
3010.493	.193E-20								6
3010.505	.393E-20								6
3010.600	.231E-20								6
3010.673	.512E-20								6
3010.747	.740E-20								6
3010.803	.357E-20								6
3010.880	.161E-19								6
3010.903	.173E-19								6
3011.241	.290E-20								6
3011.435	.457E-19								6
3011.597	.730E-20								6
3011.694	.323E-20								6
3011.739	.287E-20								6
3011.819	.964E-20								6
3011.929	.384E-20								6
3012.023	.104E-19								6
3012.052	.804E-20								6
3012.229	.101E-19								6
3012.502	.472E-20								6
3012.616	.133E-18								6
3012.715	.492E-20								6
3012.794	.343E-20								6
3012.839	.139E+20								6
3012.853	.620E-20								6
3012.916	.740E+20								6
3013.077	.104E-19	689.342	00	11001	00000000	1111A11	1111A21	36 211	6
3013.127	.232E-19	689.377	00	11001	00000000	1111F12	1111F22	36 211	6
3013.161	.281E-19								6
3013.409	.883E-20	815.110	00	11001	00000000	1212F11	1212F21	36 211	6
3013.517	.881E-20	815.132	00	11001	00000000	1212F21	1212F11	36 211	6
3013.542	.150E-19	815.144	00	11001	00000000	1212A21	1212A11	36 211	6
3013.806	.103E-19	689.957	00	11001	00000000	1111F22	1111F12	36 211	6
3014.056	.208E-19	690.018	00	11001	00000000	1111F13	1111F23	36 211	6
3014.097	.203E-19	575.170	00	11001	00000000	1010F12	1010F22	36 211	6
3014.171	.191E-19	575.184	00	11001	00000000	1010F22	1010F12	36 211	6
3014.276	.111E-19	690.040	00	11001	00000000	1111 E2	1111 E2	36 211	6
3014.344	.242E-19	690.049	00	11001	00000000	1111F23	1111F13	36 211	6
3014.641	.251E-19	575.223	00	11001	00000000	1010A21	1010A11	36 211	6
3014.713	.140E-18	376.730	00	11001	00000000	8 8A21	8 8A11	36 211	6
3014.833	.173E-19	575.246	00	11001	00000000	1010F21	1010F11	36 211	6
3014.941	.258E-19	575.272	00	11001	00000000	1010 E1	1010 E1	36 211	6
3015.001	.163E-19	470.709	00	11001	00000000	9 9 E1	9 9 E1	36 211	6
3015.05[illegible]	.28[illegible]E-19	470.815	00	11001	00000000	9 9F22	9 9F12	36 211	6
3015.09[illegible]	.177E-19	575.235	00	11001	00000000	1010F11	1010F21	36 211	6
3015.202	.513E-19	470.831	00	11001	00000000	9 9A21	9 9A11	36 211	6
3015.589	.263E-19	470.855	00	11001	00000000	9 9F23	9 9F13	36 211	6
3015.641	.383E-20	293.123	00	11001	00000000	7 7F21	7 7F11	36 211	6
3015.694	.927E-19	293.126	00	11001	00000000	7 7F11	7 7F21	36 211	6
3015.988	.501E-19	376.835	00	11001	00000000	8 8F21	8 8F11	36 211	6
3016.301	.263E-19	376.521	00	11001	00000000	8 8 E1	8 8 E1	36 211	6

Table 2. Results Obtained (Cont)

3016.369	.383E-19	376.836	00	11001	00000000	8 8F11	5 8F21	36	211	6
3016.458	.590E-19	219.913	00	11001	00000000	6 6 E1	5 6 E1	36	211	6
3016.565	.147E-18	219.920	00	11001	00000000	6 6A11	5 6A21	36	211	5
3016.648	.614E-19	293.164	00	11001	00000000	7 7F12	7 7F22	36	211	5
3016.733	.447E-19	293.170	00	11001	00000000	7 7 E1	7 7 E1	36	211	5
3016.945	.710E-19	293.178	00	11001	00000000	7 7F22	7 7F12	36	211	5
3017.163	.898E-19	157.124	00	11001	00000000	5 5F21	5 5F11	36	211	5
3017.228	.877E-19	219.937	00	11001	00000000	6 6F11	5 6F21	36	211	5
3017.266	.102E-18	157.128	00	11001	00000000	5 5F11	5 5F21	36	211	5
3017.346	.800E-19	219.911	00	11001	00000000	6 6F21	5 6F11	36	211	6
3017.467	.142E-18	219.945	00	11001	00000000	6 6A21	5 6A11	36	211	6
3017.711	.992E-19	104.773	00	11001	00000000	4 4A21	4 4A11	36	211	5
3017.763	.411E-19	157.137	00	11001	00000000	5 5 E1	5 5 E1	36	211	5
3017.886	.499E-19	104.776	00	11001	00000000	4 4 E1	4 4 E1	36	211	5
3018.205	.110E-18	104.780	00	11001	00000000	4 4F11	4 4F21	36	211	5
3018.241	.102E-18	62.876	00	11001	00000000	3 3F21	3 3F11	36	211	5
3018.358	.109E-18	62.877	00	11001	00000000	3 3F11	3 3F21	36	211	5
3018.528	.135E-18	62.878	00	11001	00000000	3 3A11	3 3A21	36	211	5
3018.591	.454E-19	31.442	00	11001	00000000	2 2 E1	2 2 E1	36	211	5
3018.656	.773E-19	31.442	00	11001	00000000	2 2F11	2 2F21	36	211	6
3018.824	.535E-19	10.482	00	11001	00000000	1 1F21	1 1F11	36	211	6
3019.002	.557E-21	0.0 0	00	11001	00000000	1 0A21	0 0A11	36	311	6
3020.373	.105E-21	31.440	00	11001	00000000	2 3F11	2 2F21	73	211	5
3020.391	.329E-21	615.054	00	11001	00000000	1213A11	1212A21	73	211	6
3020.465	.275E-21	684.830	00	11001	00000000	1112A11	1111A21	73	211	5
3020.557	.494E-21	62.872	00	11001	00000000	3 4F11	3 3F21	73	211	6
3020.665	.220E-21	575.151	00	11001	00000000	1011F13	1010F22	73	211	6
3020.748	.220E-21	689.980	00	11001	00000000	1112F12	1111F23	73	211	5
3020.772	.165E-21	475.773	00	11001	00000000	910 E2	9 9 E1	73	211	6
3020.772	.439E-21	104.757	00	11001	00000000	4 5F22	4 4F11	73	211	5
3020.802	.110E-21	470.839	00	11001	00000000	910F22	9 9F13	73	211	6
3020.819	.165E-21	62.871	00	11001	00000000	3 4F21	3 3F11	73	211	5
3020.835	.714E-21	104.760	00	11001	00000000	4 5 E1	4 4 E1	73	211	5
3020.861	.165E-21	376.763	00	11001	00000000	8 9F12	8 8F21	73	211	5
3020.893	.165E-21	293.146	00	11001	00000000	7 8F12	7 7F22	73	211	5
3020.893	.165E-21	689.345	00	11001	00000000	1112F12	1111F22	73	211	5
3020.906	.275E-21	219.926	00	11001	00000000	6 7F22	5 6F11	73	211	5
3020.938	.439E-21	376.782	00	11001	00000000	8 9F23	8 8F12	73	211	5
3020.939	.494E-21	157.113	00	11001	00000000	5 6F21	5 5F11	73	211	5
3020.966	.384E-21	293.151	00	11001	00000000	7 8 E2	7 7 E1	73	211	6
3020.982	.275E-21	575.231	00	11001	00000000	1011F22	1010F12	73	211	5
3021.013	.110E-21	376.781	00	11001	00000000	8 9F22	8 8F11	73	211	6
3021.044	.124E-20	157.136	00	11001	00000000	5 6F11	5 5F21	73	211	5
3021.057	.494E-21	219.898	00	11001	00000000	6 7 E1	5 6 E1	73	211	6
3021.147	.154E-20	470.835	00	11001	00000000	910A21	9 9A11	73	211	5
3021.161	.824E-21	219.930	00	11001	00000000	6 7F11	5 6F21	73	211	5
3021.179	.110E-20	376.788	00	11001	00000000	8 9A21	8 8A11	73	211	6
3021.179	.769E-21	293.174	00	11001	00000000	7 8F22	7 7F11	73	211	5
3021.204	.105E-21	104.747	00	11001	00000000	4 5F21	4 4F11	73	211	5
3021.273	.275E-21	614.516	00	11001	00000000	1213A21	1212A11	73	211	5
3021.299	.220E-21	470.829	00	11001	00000000	910F21	9 9F13	73	211	5
3021.346	.297E-20	219.964	00	11001	00000000	6 7A11	5 6A21	73	211	6
3021.378	.439E-21	293.140	00	11001	00000000	7 8F21	7 7F12	73	211	5
3021.378	.439E-21	376.792	00	11001	00000000	8 9F22	8 8F12	73	211	5
3021.383	.275E-21	689.571	00	11001	00000000	1112F22	1111F11	73	211	5
3021.431	.104E-20	293.1 7	00	11001	00000000	7 8F11	7 7F21	73	211	6
3021.441	.494E-21	470.541	00	11001	00000000	910F21	9 9F11	73	211	5
3021.441	.714E-21	376.771	00	11001	00000000	8 9F22	8 8F11	73	211	6
3021.459	.275E-21	684.573	00	11001	00000000	1112F11	1111F21	73	211	6
3021.479	.439E-21	575.042	00	11001	00000000	1011F12	1010F21	73	211	5

Table 2. Results Obtained (Cont)

3021.495	.604E-21	37[illegible].713	00	11001	00000000	8 9 E1	8 8 E1	73	211	6
3021.52[illegible]	.657E-21	47[illegible].544	00	11001	00000000	910F[illegible]2	9 9F21	73	211	6
3021.545	.864E-21	575.0[illegible]5	00	11001	00000000	1011A[illegible]1	1010A21	73	211	6
3024.722	.127E-20									6
3024.739	.41[illegible]E-2[illegible]									6
3025.76[illegible]	.137E-20									6
3028.755	.874E-19	[illegible]	00	11001	00000000	1 0A21	0 0A11	36	211	6
3030.725	.147E-20									6
3031.733	.172E-20									6
3031.991	.480E-21									6
3032.065	.400E-21									6
3034.264	.145E-20									6
3038.12[illegible]	.215E-21									6
3038.498	.972E-19	1[illegible].4[illegible]2	00	11001	00000000	2 1F21	1 1F11	36	211	6
3042.40[illegible]	.200E-21									6
3057.586	.857E-19	52.378	00	11001	00000000	4 3A11	3 3A21	36	211	6
3057.751	.117E-18	52.370	00	11001	00000000	4 3F21	3 3F11	36	211	6
3057.913	.115E-20	104.770	00	11001	00000000	5 4 E1	4 4 E1	36	311	6
3057.962	.125E-20	104.773	00	11001	00000000	5 4A[illegible]1	4 4A11	36	311	6
3067.163	.105E-18	104.7[illegible]0	00	11001	00000000	5 4F11	4 4F21	36	211	6
3067.236	.45[illegible]E-19	104.770	00	11001	00000000	5 4 E1	4 4 E1	36	211	6
3067.25[illegible]	.175E-18	104.775	00	11001	00000000	5 4F21	4 4F11	36	211	6
3067.249	.117E-18	104.773	00	11001	00000000	5 4A21	4 4A11	36	211	6
3067.457	.160E-20	157.128	00	11001	00000000	6 5F11	5 5F21	36	311	6
3076.075	.912E-19	157.128	00	11001	00000000	6 5F11	5 5F21	36	211	6
3076.72[illegible]	.118E-18	157.124	00	11001	00000000	6 5F21	5 5F11	36	211	6
3076.907	.106E-20	219.9[illegible]0	00	11001	00000000	7 6A11	6 6A21	36	311	6

Table 3. The Lines Unanalyzed Because of a Severe Blending

2917.653	00011001	00000000	910F13	1010F23	211
2917.662	00011001	00000000	910 E2	1010 E2	211
3013.711	00011001	00000000	9 9F21	9 9F11	211
3013.724	00011001	00000000	9 9F11	9 9F21	211
3014.735	00011001	00000000	8 8F22	8 8F11	211
3014.746	00011001	00000000	8 8 E2	8 8 E2	211
3017.815	00011001	00000000	4 4F21	4 4F11	211
3017.825	00011001	00000000	5 5F22	5 5F12	211
3048.153	00011001	00000000	3 2 E1	2 2 E1	211
3048.169	00011001	00000000	3 2F11	2 2F21	211

References

1. McClatchey et al (1973) AFCRL Atmospheric Absorption Line Parameters Compilation, AFCRL-TR-73-0096.
2. Fox, K. (1973) Analysis of Vibration-Rotation Spectra of Methane, AFCRL-TR-73-0738.
3. Pritchard et al (1973) Two-Meter Path Difference Interferometer for Fourier Spectroscopy, AFCRL-TR-73-0223.
4. Sakai, H. (1974) High-Resolution Fourier Spectroscopy, AFCRL-TR-74-0571.
5. Tarrago et al (1976) J. Mol. Spectrosc., 57:246.
6. Pine, A.S. (1976) J. Opt. Soc. Am., 66:97.